BULLETIN OF THE CHEMICAL SOCIETY OF JAPAN VOL. 43 663—669 (1970)

Measurement of the Hydrogen Ion Concentration in the Vicinity of the Anode during Electrodeposition of Water-Soluble Resin*1

Yoshio NAKAMURA, Kimio KOMATA and Hiroshi NOZAKI

Institute of Industrial Science, The University of Tokyo Roppongi, Minato-ku, Tokyo

(Received August 4, 1969)

In order to make clear the mechanism of the electrodeposition of water-soluble resin, the hydrogen ion concentration in the vicinity of the anode during electrodeposition was measured using a quinhydrone reaction on platinum wire. The measured concentration of hydrogen ions in the vicinity of the anode was then compared with that of hydrogen ions which had been calculated according to the diffusion theory. The results show that the most of the hydrogen ions produced at the anode during electodeposition are consumed in the vicinity of the anode. This shows that there is apparently ionic combination of hydrogen ions with organic anions on the anode; this may lead to the deposition of organic anions.

Many reports related to the mechanism of the electrodeposition of water-soluble resin have been published. For example, the results of the analyses of the gas generated at the anode during electrodeposition,[1-3] chemical analyses of the components of the deposited film,[4-6] and electrochemical interpretations of electrode phenomena[2,5,7] have been reported. These reports have supported the idea that the film formation of water-soluble resin is made by coagulation caused by the ionic combination of anionic resin with hydrogen ions according to the following reaction:

$$R(COO^-)_n + nH^+ = R(COOH)n \qquad (1)$$

where $R(COO^-)_n$ represents the organic anion.

Moreover, a current-time relation was observed at a constant voltage deposition, and results which may support the coagulation theory were obtained.[8]

These reports show that the principal electrode reaction at the anode during the electrodeposition of water-soluble resin is the electrolysis of water, which gives hydrogen ions at the anode; these ions then cause the coagulation of organic anions. Therefore, one of the best means to make clear the mechanism of the film formation is the measurement of the concentration of hydrogen ions on the anode surface. However, this measurement is very difficult because the diameter of the glass electrode is not small enough to measure the concentration gradient of hydrogen ions on the anode. Nevertheless, even the results were not rigorous, at first, the concentration gradient of hydrogen ions on the anode was measured using indicating reagents.

In order to obtain detailed results, the concentration of hydrogen ions in the vicinity of the anode was measured using a quinhydrone reaction on the platinum wire; some appreciable results were thus obtained.

Experimental

Sample. Maleic methyleleostearate was used as a water-soluble resin. Methyleleostearate was obtained by the methyl-inter-esterification of china wood oil. A mixture of 150 g of methyleleostearate and 50 g of maleic anhydride was heated for two hours at 180°C and then for additional three hours at 230°C. During the reaction, the mixture was kept in a nitrogen atomosphere. The method of purifying the reaction product was the same as that reported in a previous report.[8] The purified maleic methyleleostearate was dissolved into potassium hydroxide solution, after which this solution was used as a sample. The pH of the solution was adjusted by means only of the potassium hydroxide solution and maleic methyleleostearate. We name this solution simply the MME solution.

The potassium chloride, quinhydrone, and hydroquinone used in this experiment were of a special grade.

Apparatus. The measurement of the pH in the vicinity of the anode was made by means of measuring the potential of the hydroquinone-quinone reaction on platinum wire, as is shown in Fig. 1 (A).

*1 Electrodeposition of Water-Soluble Resin VI.

1) L. R. L. Brass, *J. Paint Technol.*, **38**, 493 (1966).

2) Y. Nakamura, N. Higashiyama and H. Nozaki, *Denki Kagaku*, **36**, 278 (1968); Y. Nakamura, S. Ando and H. Nozaki, *J. Electrochem. Soc. Jap.*, **37**, 13 (1969).

3) S. Yoshizawa, N. Watanabe, I. Tari and I. Totake, 34th Conference of the Electrochemical Soc. of Japan.

4) M. R. Sullivan, *J. Paint Technol.*, **38**, 424 (1966).

5) S. Maeda, N. Hirai, H. Okada and K. Inoue, *Denki Kagaku*, **34**, 705 (1966).

6) T. Nakamura, M. Nagasawa and I. Kagawa, *J. Ind. Chem.* (Japan), **70**, 2 (1967).

7) S. R. Finn, C. C. Mell, *J.O.C.C.A.*, **41**, 219 (1964); A. R. H. Tawn and J. R. Berry, *ibid.*, **28**, 790 (1965), *etc.*

8) Y. Nakamura, H. Oki and H. Nozaki, This Bulletin, **42**, 1534 (1969).

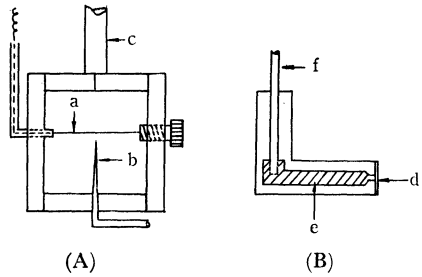

Fig. 1. Platinum wire electrode (A) and electrolysis electrode (B).
a: platinum wire, b: capillary electrolyte bridge, c: arm, d: platinum plate electrode, e: mercury, f: copper rod.

The platinum wire had a diameter of 0.05 mm, all its surface except for a length of 5 mm was insulated by organic resin. The arm of the frame which supported the platinum wire electrode was supported by the arm of the cathetometer. The platinum electrolysis electrode is shown in Fig. 1(B). A polished platinum plate was stuck on the even frame and connected to the copper rod through the mercury pool. The frames of both (A) and (B) were made of acrylic resin. As is shown in Fig. 2, a microscope was arranged above the electrolysis electrode and the wire electrode, so the wire electrode was set at will in the vicinity of the electrolysis electrode.

The circuits of the electrolysis and the measurement of the quinhydrone electrode potential are shown in Fig. 2.

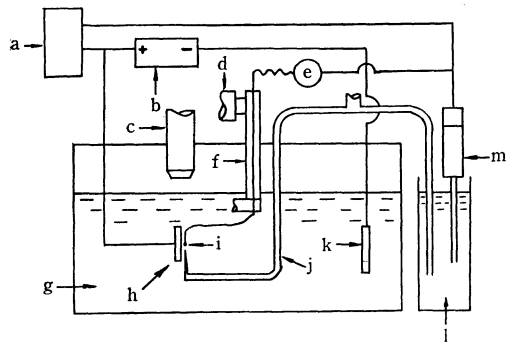

Fig. 2. Circuits of electrolysis and measurement of Q.H. potential.
a: XY recorder, b: current supply, c: microscope, d: arm of cathetometer, e: electrometer, f: arm of wire electrode, g: electrolyte solution, h: platinum plate, i: platinum wire electrode, j: electrolyte bridge, k: cathode, l: saturated KCl solution, m: saturated calomel electrode.

During electrolysis, the electrolysis electrode potential (=anode potential) was recorded by means of a Riken Denshi XY recorder, model F-42. The quinhydrone potential was measured by means of a Keysley electrometer, model 610B. This measurement was made when the electrolysis circuit was open in order to escape the $i \cdot R$ effects, where i and R are the current and the resistance of the electrolyte solution respectively. The quinhydrone potential was measured within 2 sec. However, when the electrolyte solution was a 1N KCl solution saturated with quinhydrone, the quinhydrone potential was measured without cutting the current. We will abbreviate hydroquinone, quinone and quinhydrone H.Q., Q., and Q.H. respectively.

When Q.H. was added to the electrolyte solution, H.Q. was oxidized at the anode as follows:

$$C_6H_4(OH)_2 \rightleftarrows C_6H_4O_2 + 2H^+ + 2e \qquad (2)$$

Then the anode reaction of the electrolyte solution saturated with Q.H. was observed. The pH of the anode part of the cell, which is shown in Fig. 3, was measured.

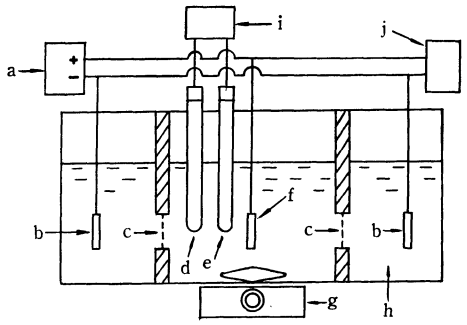

Fig. 3. Apparatus for pH measurement of anode part.
a: current supply, b: cathode, c: milipore filter, d: calomel electrode, e: glass electrode, f: anode, g: stirrer, h: electrolyte solution, i: pH meter, j: XY recorder.

The anode part and the cathode parts of the cell were separated by milipore filters. When a electrolyte solution including a supporting electrolyte is used, most hydrogen ions produced at the anode remain within the anode part because the migration and diffusion of the hydrogen ions into the cathode parts are negligible compared with their production rate. The cells shown in Figs. 2 and 3 were kept 25±0.5°C.

Results

Hydrogen Ion Production at the Anode. The mechanism of the deposition of water-soluble resin is considered to be a coagulation of organic anions occuring by means of ionic combination with hydrogen ions, so the anode reaction of the aqueous electrolyte solution saturated with Q.H. must also be investigated.

Using the cell shown in Fig. 3, the pHs of the anode part during the constant-current electrolysis of a 1N KCl solution and a 1N KCl solution saturated with Q.H.*2 were measured. The results are shown in Fig. 4, which shows that the rate of the production of hydrogen ions is nearly the same whether the electrolyte solution includes Q.H. or

*2 An oversaturated solid substance of Q.H. was filtered out at 25°C.

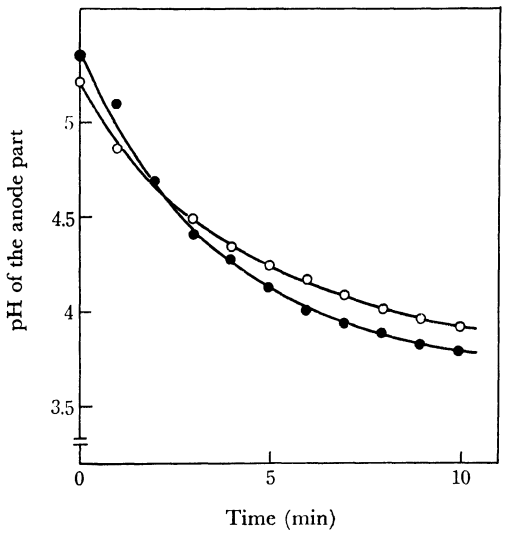

Fig. 4. pH of the anode part against time.
●: 1N KCl solution saturated with Q.H., ○: 1N KCl solution, current density 2.5 mA/cm².

not.

However, the anode potentials during electrolysis were about 0.45 and 1.1 V (*vs.* SCE) in the cases of a 1N KCl solution saturated with Q.H. and a 1N KCl solution respectively. These results can naturally be expected according to Reactions (2), (3), and (4):

$$4OH^- = 2H_2O + O_2 + 4e \quad (3)$$

$$2H_2O = 4H^+ + O_2 + 4e \quad (4)$$

Moreover, the effects on the deposition of the addition of Q.H. to the deposition bath (5% in-weight MME solution) were observed; the results are shown in Table 1, where τ_2 is the transition time as shown in Fig. 9. It is known that after $t=\tau_2$ an organic film is formed on the anode.

Table 1. Effects of the concentration of Q.H. on transition time τ_2 (sec)

Current density (mA/cm²)	Concentration of Q.H. (mol/l)·10²		
	0	0.9	2.0
2.5	86	80	75
5.0	21	20.5	20

The results show that τ_2 decreased as the weight of the addition of Q.H. increased, but the effect was minor.

pH and Q.H. Electrode Potential. The equilibrium potential of Q.H. solution is given by Eq. (5) according to Reaction (2):

$$E = E_0 + (RT/2F)\ln(a_{Q.}/a_{H.Q.}) + (RT/F)\ln a_{H^+} \quad (5)$$

where E, E_0, and a_i are measured potential, the standard potential, and the activity of the i species respectively. As the concentration of Q. equals that of H.Q. in the bulk solution, according to Eq. (6), the second term on the right-hand side of Eq. (5) is zero.

$$C_6H_4(OH)_2 \cdot C_6H_4O_2 = C_6H_4(OH)_2 + C_6H_4O_2 \quad (6)$$

Here we name the second term E_1. However, when the Q.H. electrode potential was measured in the vicinity of the anode where the current flows, the second term (E_1) is not zero but a function of x, t, and I, where x, t, and I are the distance from the anode surface, the time after switch-on, and the current density respectively.

The relations between the pH and the Q.H. equilibrium potential are shown in Fig. 5.

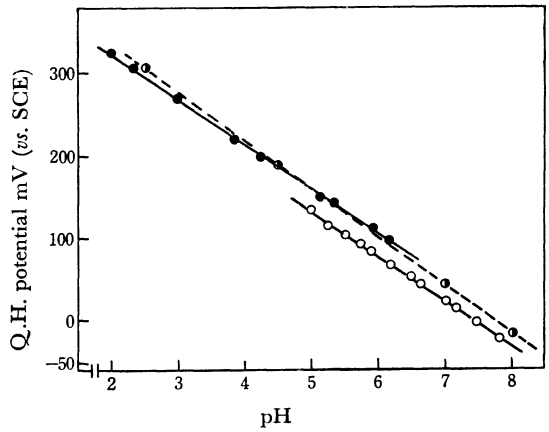

Fig. 5. Q.H. potential against pH.
●: 1N KCl solution, ○: MME solution, ◑: theoretical curve.

The potential was measured at 25°C using a saturated calomel electrode as the reference electrode. The pH was measured by means of a Hitachi-Horiba pH meter, model 5. The pH of the solution was adjusted by means of the addition of hydrogen chloride solution. The same figure also shows theoretical curve given by Eq. (5). The potential-pH curve of a 1N KCl solution differs from that of the 5% (in weight) MME solution.

However, the linear relation between the potential and the pH is satisfied in both solutions, and the values of the slopes of the curves are nearly equal. In the MME solution, a plot of the potential against the same value of pH gradually decreased with time, but the linearity between potential and pH was satisfied at all times and the value of the slope of the line was kept constant. Therefore, by measuring a potential against a value of pH, the relation between potential and pH was obtained as a function of the time.

Electrolysis of KCl Solution and pH Measurements. In order to test the method, the pH in the vicinity of the anode was measured by means of Q.H. potential measurement and was

compared with the results of theoretical calculation. The electrolyte solution was a 1N KCl solution saturated with Q.H.

In Fig. 6, the measured potential at $x=0.1$ mm is shown; the anode potential is also shown in Fig. 6.

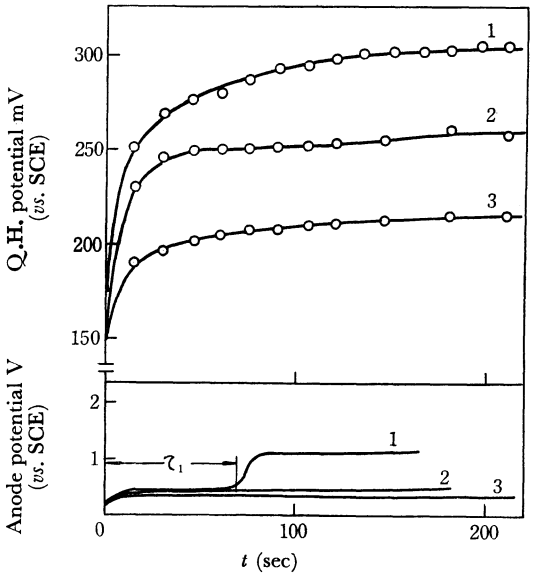

Fig. 6. Q.H. potential at $x=0.1$ mm and anode potential against time in 1N KCl solution saturated with Q.H. current density, 1 : 1.0, 2 : 0.1, 3 : 0.01 mA/cm².

In the range of current density from 0.01 to 0.1 mA/cm², the anode potential during electrolysis was kept about 0.4—0.6 V (*vs.* SCE). However, when the current density was 1 mA/cm², the transition to a more noble potential was observed; we term this transition time τ_1.

The values of the Q.H. potential shown in Fig. 6 were converted to the pH value using the results shown in Fig. 5, and the pH-time curves are shown in Fig. 7. In a solution containing a supporting electrolyte, hydrogen ions produced at the anode will diffuse to the bulk solution from the anode surface. Therefore, it is possible to calculate the hydrogen ion concentration or pH as a function of x, t, and I.[9]

Assuming that the diffusion is one dimension and that the reaction shown in Eq. (2) or (4) occurs at the anode, the values of pH in the vicinity of the anode were calculated; the results are also shown in Fig. 7. The chemical reaction of hydrogen ions and hydroxide ions is negligible when the pH of the electrolyte solution is smaller than 6. Figure 7

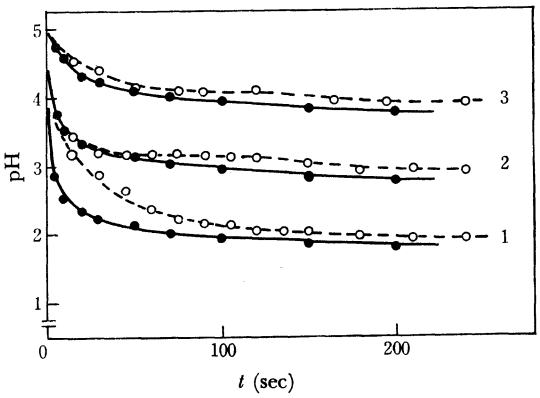

Fig. 7. pH at $x=0.1$ mm against time in 1N KCl solution saturated with Q.H. current density, 1 : 1.0, 2 : 0.1, 3 : 0.01 mA/cm², the dotted lines are experimental curves and the solid lines are theoretical curves.

shows that this method of pH measurement is reproducible, though it is not highly accurate.

Electrodeposition and pH Measurement. Electrodeposition was made at a constant current density. The concentration of MME was 5% (in weight), and the pH of the MME solution was 7.9. The Q.H. potential during deposition was measured, after which the values were converted to the pH values. In Fig. 8, the pH values at $x=0.1$, 0.2, and 0.5 mm are shown against the time after the current has been put on. The dotted line drawn in Fig. 8 shows that film formation begins at that time, that is, $t=\tau_2$.

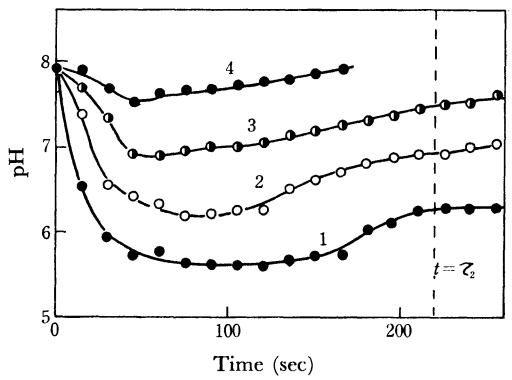

Fig. 8. pH against time.
Current density 2 mA/cm², MME concentration 2.5% (in weight), x, 1 : 0.1, 2 : 0.2, 3 : 0.3, 4 : 0.5 mm.

Deposition was made at several concentration of MME but at a constant current density, 3 mA/cm², and the potential of Q.H. at $x=0.3$ mm was measured. The pHs of the solution were adjusted to 7.9. The results, converted to the pH values are shown in Fig. 9. The anode potentials are also shown in Fig. 9.

9) P. Delahay, "New Instrumental Method in Eelctrochemistry," Interscience Pub. (1954), p. 47; H. S. Carslaw and J. C. Jaeger, "Conduction of Heat in Solids," Clarendon Press (1950), p. 216.

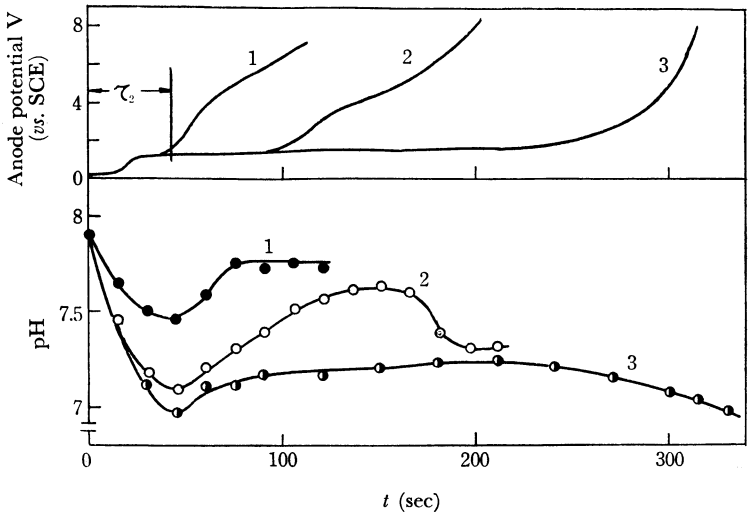

Fig. 9. Anode potential and pH at x=0.3 mm against time.
MME concentration, 1 : 5, 2 : 2.5, 3 : 1.25% (in weight), current density 3 mA/cm².

τ_2 increases with a decrease in the concentration of MME. On the other hand, the values of pH decrease with an increase in the concentration of MME, and the curves of pH and time have a peak.

The Q.H. potential at several concentrations of MME was measured as a function of x, and t; the values of the potential were then converted to the pH values by using the results shown in Fig. 5. The values of pH at t=20 and 75 sec are shown against x in Figs. 10 and 11 respectively. The theoretical values of the pH calculated as before are also plotted in these figures. They show that the concentration of hydrogen ions in the vicinity of the anode is smaller than that of the hydrogen ions which were calculated theoretically.

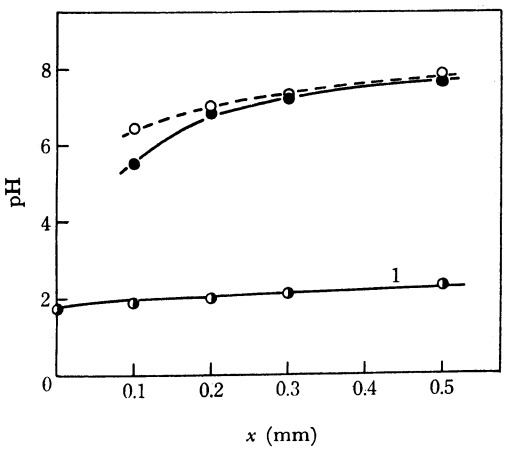

Fig. 10. pH at t=20 sec against x.
Current density 3 mA/cm², MME concentration, ●: 2.5, ○: 5% (in weight), pH of the bulk solution is 7.9, 1: theoretical curve.

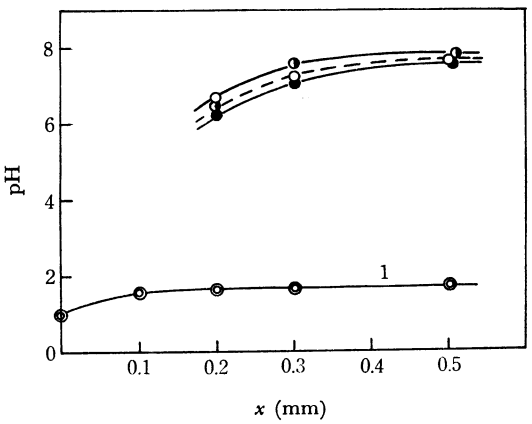

Fig. 11. pH at t=75 sec against x.
Current density 3 mA/cm², MME concentration, ●: 1.25, ○: 2.5, ◑: 5% (in weight), 1: theoretical curve.

Discussion

When the potential of the reaction shown in Eq. (2) in the vicinity of the anode, where the current flow is measured, the concentration of H.Q. decreases and that of Q. increases in the solution. This causes the E_1 potential. By means of chronopotentiometry, the saturated concentration of Q.H. was measured. $I \cdot \tau_1^{1/2}$ was plotted against the concentration of Q.H. in 1N KCl solution and 5% (in weight) MME solution. Moreover, $I \cdot \tau_1^{1/2}$ was plotted against the concentration of H.Q. in a 1N KCl solution. The results, shown in Fig. 12, show that the concentration of H.Q. is nearly equal to that of Q.H. when Q.H. is dissolved in the solution.

Table 2. Calculated E_1 (mV) at low current density

I (mA/cm²)	x(mm)	(t sec) 5	10	15	20	30	50	70	100	150	200
0.5	0.1	0.5	1.8	2.5	3.6	4.4	6.4	10	13	19	25
	0.2	—	0.3	1.0	1.3	1.6	4.2	6.5	8.7	13	16
	0.3	—	—	—	—	0.8	2.1	3.5	6.2	8.8	12
	0.5	—	—	—	—	—	0.4	0.9	2.0	3.8	6.3
1.0	0.1	1.2	3.3	5.1	7.7	8.2	17	24	(50)		
	0.2	—	0.7	2.1	2.4	3.3	7.8	13	(20)		
	0.3	—	—	0.6	0.7	1.0	4.3	7.4	(12)		
	0.5	—	—	—	—	—	0.9	2.0	(4.0)		

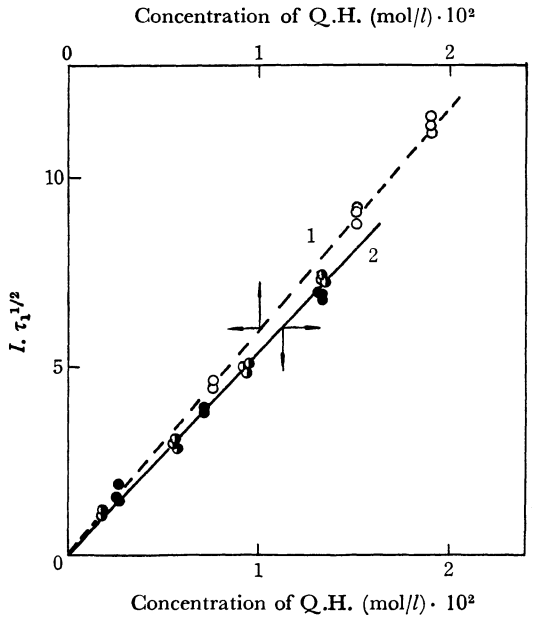

Fig. 12. $I\cdot\tau_1^{1/2}$ against concentration of Q.H. or H.Q.
1: when H.Q. was dissolved into 1N KCl solution,
2: when Q.H. was dissolved into, ●: 5% MME solutionl ◑: 1N KCl solution.

That is, most of the dissolved Q.H. dissociates to H.Q. and Q. From the $I\cdot\tau_1^{1/2}$ values of the saturated solution and the results shown in Fig. 12, the saturated concentrations of Q.H. were found to be about 1.5×10^{-2} and 2.1×10^{-2} mol/l in the 1N KCl solution and in the 5% (in weight) MME solution respectively.

Assuming that the reaction shown in Eq. (2) occurs at a constant current density, I, and that H.Q. and Q. are transported only by diffusion with one dimension, their concentrations can be calculated as functions of x, t, and I. Then, if $C_i(x,t)=a_i(x,t)$, E_1 can be calculated according to Eq. (5), where $C_i(x,t)$ means the concentration at x and t of the i species. In Table 2, the values of E_1 are shown as functions of x, t, and I. The values of E_1 were calculated assuming that $D_{Q.}=D_{H.Q.}$*3 and $(dC_{Q.}(x,t)/dX)_{x=0}+(dC_{H.Q.}(x,t)/dX)_{x=0}=0$.

$I\cdot\tau_1^{1/2}$ in a 1N KCl solution saturated with Q.H. is about 8.5. Therefore, when the current densities are from 0.01 to 0.1 mA/cm², the transition from the oxidation of H.Q. to that of water does not occur within 200 sec, and the value of E_1 is negligibly small compared with the values of the other term in Eq. (5). When the current density is larger than 0.5 mA/cm², E_1 becomes appreciable with the time, as is shown in Table 2, and the transition occurs as is shown in Figs. 6 and 9. In Table 2, the values of E_1 at $I=1.0$ mA/cm² and $t=100$ sec are not obvious because the transition occurs at 75 sec.

However, as is shown in Figs. 8 and 9, the Q.H. potential does not increase so much with the time. After the transition has occurred, the anode reaction will be the reaction shown in Eqs. (3) and (4), so Reaction (2) may be retrained by Reaction (3) and (4).

In the case of high current densities, the approximate concentrations of H.Q. and Q. will be given as follows. When the current density is high, τ_1 becomes very short, so it may be assumed that at $t=0$, the initial concentration of H.Q. at $x=0$ is zero and that the initial concentration of Q. equal to that of H.Q. at $x\neq0$. According to the diffusion theory, the concentrations of H.Q. and Q. were calculated as functions of x and t, and the values of E_1 were calculated. The results are shown in Table 3.

Table 3 shows that, within $t=200$ sec, the value of E_1 is 30 mV at most; this value corresponds the pH value of 0.5, according to Fig. 5. It is considered that the peak of the pH-time curve in Fig. 9 is caused by E_1 and the transition from the oxidation of H.Q. to that of water, for the pH-time curves in Figs. 7—11 were obtained from the value of the

*3 $D_{H.Q.}$ is the diffusion constant of H.Q.; it has value of 7.6×10^{-6} cm²/sec at 25°C.[10]

10) International Critical Table, Vol. 70 (1933); M. Kolthoff and E. F. Lingane, *J. Amer. Chem. Soc.*, **63**, 664 (1941).

TABLE 3. CALCULATED E_1 (mV) AT HIGH CURRENT DENSITY

x (mm)	t (sec)									
	5	10	15	20	30	50	70	100	150	200
0.1	4.0	13	16	18	21	24	28	30	32	34
0.2	1.4	3.6	5.9	7.6	11	14	17	21	23	24
0.3	—	1.0	1.8	4.9	5.2	8.5	12	15	17	18
0.5	—	—	—	—	0.8	2.5	4.5	7.5	10	11

measured Q.H. potential without any correction for E_1. However, the transition time, τ_1, does not correspond to the time at which a peak appears. At present, it is not obvious why a peak appears on the pH-time curve.

As is shown in Figs. 8 and 9, the hydrogen ion concentration in the vicinity of the anode does not increase with the time, but remains lower than the concentration to be expected from only the diffusion process. That is, most hydrogen ions produced at the anode are consumed on the anode surface. This shows that there is an ionic combination of hydrogen ions with MME anions. In Fig. 9, some anode potential-time curves are shown, and the transition time, τ_2, is observed on the curves. As has been noted previously, τ_2 shows that film formation begins. Compared with the pH-time curve, it is found that the rate of the ionic combination of hydrogen ions on the anode does not change at all at $t=\tau_2$.

These results show that the ionic combination of hydrogen ions begins at switch-on.

In this experiment, the pH on the anode surface was not measured. Though the pH-x curves are shown in Figs. 10 and 11, it is not impossible to ascertain the value of pH on the anode surface. In the experiment of the bulk solution without an electric field, the value of pH which the MME solution begins to coagulate was about 5.